PHYSICAL REVIEW E **95**, 010201(R) (2017)

Coherent libration to coherent rotational dynamics via chimeralike states and clustering in a Josephson junction array

Arindam Mishra,[1,2,*] Suman Saha,[3,4,†] Chittaranjan Hens,[5,‡] Prodyot K. Roy,[2,6] Mridul Bose,[1] Patrick Louodop,[7,8] Hilda A. Cerdeira,[7] and Syamal K. Dana[2,9]

[1]*Department of Physics, Jadavpur University, Jadavpur, Kolkata 700032, India*
[2]*Center for Complex System Research Kolkata, Kolkata 700094, India*
[3]*Department of Electronics, Asutosh College, Kolkata 700026, India*
[4]*Dumkal Institute of Engineering and Technology, Murshidabad 742406, India*
[5]*Department of Mathematics, Bar-Ilan University, Ramat Gan 529002, Israel*
[6]*Department of Mathematics, Presidency University, Kolkata 700073, India*
[7]*Instituto de Física Teórica, Universidade Estadual Paulista, 01140-070 São Paulo, Brazil*
[8]*Department of Physics, University of Dschang, P.O. Box 67, Dschang, Cameroon*
[9]*CSIR-Indian Institute of Chemical Biology, Jadavpur, Kolkata 700032, India*

(Received 24 August 2016; revised manuscript received 16 November 2016; published 4 January 2017)

An array of excitable Josephson junctions under a global mean-field interaction and a common periodic forcing shows the emergence of two important classes of coherent dynamics, librational and rotational motion, in the weaker and stronger coupling limits, respectively, with transitions to chimeralike states and clustered states in the intermediate coupling range. In this numerical study, we use the Kuramoto complex order parameter and introduce two measures, a libration index and a clustering index, to characterize the dynamical regimes and their transitions and locate them in a parameter plane.

DOI: 10.1103/PhysRevE.95.010201

A surprising new phenomenon was reported in the last decade, namely, the chimera states [1–8] that emerge via a symmetry breaking of a homogeneous synchronous state in a large population of nonlocally coupled identical phase oscillators into two coexisting spatially extended coherent and noncoherent subpopulations. Presently, the existence of chimera states has been reported in identical limit cycle oscillators [8,9], chaotic systems [9–13], and very recently in excitable systems in the presence of noise [14]. It drew special attention after a similar behavior was noticed in the brain of some sleeping animals [15]. It has been now confirmed in laboratory experiments [16–18]. Most surprisingly, chimeralike states were observed in globally coupled networks of identical oscillators [19–23], which was unexpected because of the presence of a perfect symmetry in such a network. The reason for the symmetry breaking of a homogeneous state into coexisting coherent and nocoherent states still remains a puzzle.

In the meantime, more reports are coming on chimera states in many interesting systems, such as a network of neurons under different coupling forms [24], a Josephson junction array [25], and chemical oscillators [26] under nonlocal coupling, which are of practical interest. In particular, the Josephson junction, besides its main appeal as a superconducting device, shows a rich variety of dynamics, such as excitability, bistability [27–29], and neuronlike spiking and bursting [29–32], that are of common interest in other areas of nonlinear science. In fact, in the past, synchronization as a symmetry preserving phenomenon in a globally coupled Josephson junction array [33–36] was studied from the fundamental viewpoint of collective behaviors of oscillatory systems. It is now of general interest if symmetry breaking chimera states emerge in globally coupled Josephson junction arrays, too.

In this Rapid Communication, we report on the search for chimera states in a Josephson junction array under global mean-field interactions, and if they do exist, under what conditions do they occur? The existence of a state of order and turbulence was reported earlier [36] in a forced Josephson junction array under a global mean-field influence, which showed signatures of chimera states, however, no categorical statement was made at that time. We revisit that parameter space of the Josephson junction array under the same condition and confirm the existence of chimeralike states. In the process, we notice two important classes of coherent states, one regular librational motion and a regular rotational motion in the array, which are typical dynamical features [28] of a single Josephson junction. In cylindrical space [37], the trajectory of a junction is localized during a libration while it encircles the cylinder during a rotational motion (Fig. 4). Most importantly, we observe a transition between the two coherent states for changing coupling interactions. When increasing the coupling strength from a weaker range, the coherent librational motion emerges above a threshold and continues for a range of coupling, then transits to coherent rotational motion for large coupling via successive chimeralike states and clustered states in an intermediate coupling range. In the chimeralike states, we notice the coexistence of regular librational motion in a coherent subpopulation and chaotic rotational motion in another noncoherent subpopulation. In the clustered state, regular libration coexists with rotational motion in two subpopulations.

We consider an array of identical Josephson junctions when each node of the network is driven by a radio-frequency (rf) signal. We choose the global mean-field interaction for the network and identical parameters as $\alpha = 0.2$ and $I = 0.021$ for

*arindammishra@gmail.com
†ecesuman06@gmail.com
‡chittaranjanhens@gmail.com

all the junctions when an isolated junction remains in a stable steady state [29]. The set of parameters is chosen to be almost identical to what was considered earlier [36], for a revision of the past result in the search for chimera states. The rf forcing has an identical amplitude $I_{\rm rf} = 0.595$ and frequency $\Omega_{\rm rf} = 0.8$ for all the nodes that make them oscillate periodically.

The dynamics of the ith node of the rf-forced junction array is described as

$$\dot{\phi}_i = y_i, \tag{1}$$

$$\dot{y}_i = I - \sin\phi_i - \alpha y_i + I_{\rm rf}\sin(\Omega_{\rm rf} t) + K\alpha Y, \tag{2}$$

where $Y = \frac{1}{N}\sum_{j=1}^{N} y_j$ is the mean-field value of voltage $\dot{\phi}_i = y_i$ across all the junctions, $\alpha = [h/2\pi e I R^2 C]^{1/2} = (\frac{1}{\beta})^{\frac{1}{2}}$ is the damping parameter, β is the McCumber parameter, and I is the normalized constant bias current. K defines the strength of the mean-field interaction between the junctions. Increasing K reveals various network dynamics and collective states, and two coherent states, chimeralike and cluster states.

To distinguish the emergent states and their dynamics, we use the complex Kuramoto order parameter (r) [38] and introduce two measures, a clustering index (s) and a libration index (l). The complex Kuramoto order parameter r is

$$re^{i\Phi} = \frac{1}{N}\sum_{j=1}^{N} e^{i\phi_j}, \tag{3}$$

where ϕ_j is the instantaneous phase of each junction j. When all the oscillators are coherent, $r = 1$, and in an incoherent state, $r = 0$, while $0 < r < 1$ implies partial synchronization or clustering. The chimera states belong to a class of partial synchronization.

Since the order parameter r cannot distinguish the chimera states from the cluster states for intermediate values of $0 < r < 1$, we introduce a clustering index s,

$$s = \frac{\max(n)}{N}u, \tag{4}$$

where $u = 1 - \Theta(\delta_1 - d)$, $d = \max(n) - \langle n\rangle$, $\Theta(\cdot)$ is the Heaviside step function, δ_1 is an arbitrary small number, $n(t)$ is the number of distinct states counted (using a standard numerical routine) at every instant of time t in the time evolution of the network, and $\langle n\rangle$ denotes the average in a long run. The $\max(n)$ is the largest possible value of n. A clustered state (single or multiple) is now clearly distinguished by $s = 0$. It excludes a cluster state when $0 < s < 1$ but detects the existence of chimeralike states if $0 < r < 1$.

Next, the libration index l is introduced basically to characterize the dynamical features of the junctions in different collective states,

$$l = \frac{1}{N}\sum_{j=1}^{N}\Theta_j, \tag{5}$$

with $\Theta_j = \Theta(\delta_2 - m_j)$, where δ_2 is another arbitrarily chosen small threshold, $\Theta(\cdot)$ is defined above, and m_j is

$$m_j = 1 - 0.5[\max\{\cos[\phi_j(t)]\} - \min\{\cos[\phi_j(t)]\}]. \tag{6}$$

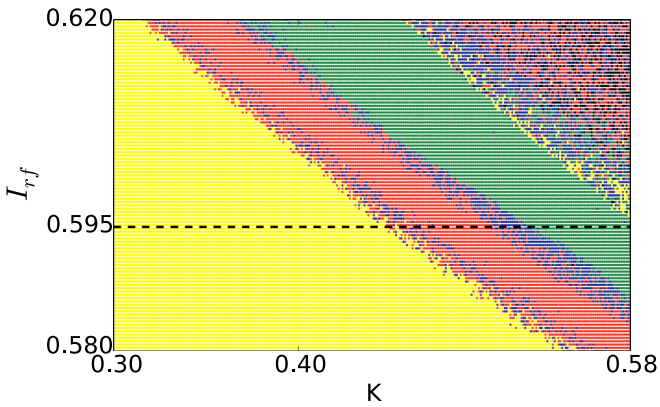

FIG. 1. Different dynamical states in $K - I_{\rm rf}$ space for $\alpha = 0.2$, $I = 0.021$, and $\Omega_{\rm rf} = 0.8$. Yellow and green regions represent coherent librational and coherent rotational motion, respectively, and blue and red regions denote cluster and chimera states, respectively. Black dots (upper corner) represent desynchronized states. We perform our numerical study in Fig. 2 along the horizontal dashed line, $I_{\rm rf} = 0.595$.

To determine m_j for the jth oscillator, we calculate $\cos[\phi_j(t)]$ for all instants of time, which vary from 0 to 2π for rotational motion when $m_j = 0$. In libration, since the trajectory of an oscillator never crosses the $\phi = \pi$ line, m_j is a positive number. Finally, it determines $l = 0$ for oscillators in libration and $l = 1$ when they are in rotational motion. A value of $0 < l < 1$ indicates the coexistence of librational and rotational motion in subpopulations of the junctions; see the Supplemental Material (SM) for details [39].

Figure 1 shows distinct dynamical regimes in the $K - I_{\rm rf}$ space where each point is plotted in color using a combination of all three of the above measures. The regions of coherent libration and coherent rotation are denoted by yellow and green colors, respectively. The red color represents chimeralike states where coherent oscillators are in libration and incoherent oscillators in rotational motion. The cluster state is depicted by the blue color where a mixed population with libration and rotation exists. Black dots represent desynchronized states. A region of messy colors is seen on the top right corner where cluster and chimera states and even coherent states coexist, which is not the focus of our current interest. As a specific example, we vary K along the horizontal dashed line ($I_{\rm rf} = 0.595$) shown in Fig. 1, and follow a transition from a coherent librational state to another coherent rotational state through the intermediate chimeralike and cluster states, as mentioned above.

Before describing further the collective dynamics, we reduce the coupled Eqs. (1) and (2) to their averaged equations (equivalent to the motion of the center of mass of our system),

$$\dot{X} = Y, \tag{7}$$

$$\dot{Y} = I - \frac{1}{N}\sum_{j=1}^{N}\sin\phi_j - (1-K)\alpha Y + I_{\rm rf}\sin(\Omega_{\rm rf} t), \tag{8}$$

where $X = \frac{1}{N}\sum_{j=1}^{N}\phi_j$ and $Y = \frac{1}{N}\sum_{j=1}^{N} y_j$ define the mean phase and mean voltage of the junction array. We

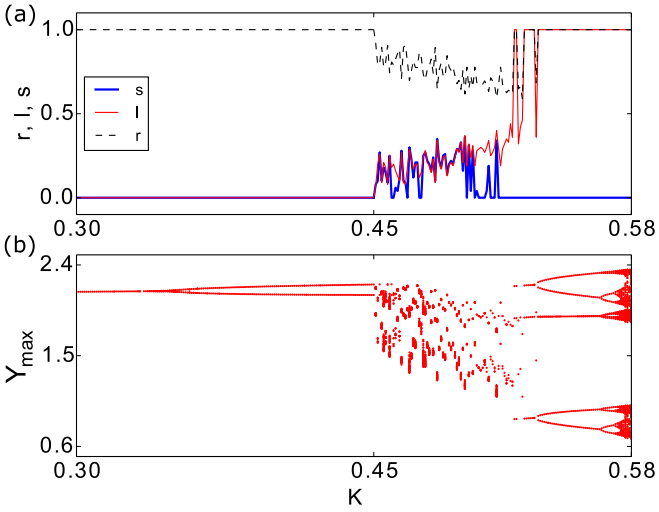

FIG. 2. Plots of r (dashed line), l (red line), and s (blue/light grey line) with coupling strength K in (a). A bifurcation plot of $Y_{\max}$ against K in (b). $\alpha = 0.2$, $I = 0.021$, $\Omega_{\rm rf} = 0.8$, $I_{\rm rf} = 0.595$.

simultaneously simulate the averaged equations and the original coupled equations. The average of $\langle \sin \phi_i \rangle$ is simulated from the original coupled equations and substituted into the averaged equation.

Figure 2(a) plots r (dashed line), s (blue/light gray line), and l (red line) for varying K in a range of 0.3–0.58. As we increase K, r becomes 1 and $s = 0$ (i.e., coherent state or single clustered state) above a threshold (not shown here) and continues for a range of coupling until r starts decreasing at a critical value, $K = 0.451$, when Y becomes chaotic. In the latter range of K values, both r and s fluctuate, $0 < r < 1$ and $0 < s < 1$, where chimeralike states emerge as a partial synchronization state. For a further increase of K above another critical value, $K = 0.512$, r starts fluctuating between 1 and intermediate values $0 < r < 1$ intermittently in small windows of K, which signifies a switching between single and multicluster states for small changes of K values until it reaches $K = 0.532$. However, $s = 0$ all along for $K > 0.512$ confirms the presence of single or multicluster states. In fact, a single cluster or a coherent state emerges at $K = 0.532$ when $r = 1$ ($s = 0$). The chimeralike states emerge only in the range of $K = 0.451$–0.512, where r shows a decreasing trend and s shows a reverse trend except in the clustered states (small windows of single clusters and multicluster states).

Figure 2(b) presents a bifurcation diagram of $Y_{\max}$ with K. It reveals that the collective dynamics in the left coherent region (cf. upper panel) bifurcates from a single period to period-2 and larger periods, and is followed by chaos in the chimera region. In this chimera region, the $Y_{\max}$ plot indicates chaotic behavior where the average Y was taken on two subpopulations, one in coherent periodic motion and another in noncoherent chaotic motion. A small window of multiclustered states (period-3) exists immediately after the chimera region, followed by single cluster higher periodic rotational orbits (period-6) on the right (lower panel), that again bifurcates via period doubling to chaos, however, remaining in a coherent rotational state. Note that r, s, and l do not fluctuate here, which distinguishes it from the chaotic chimera states.

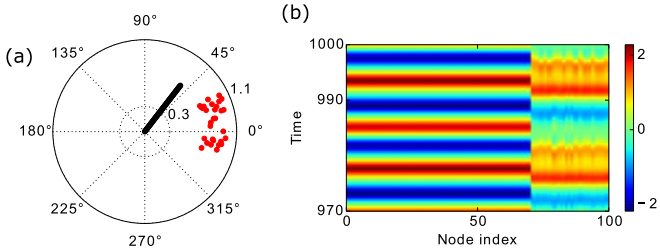

FIG. 3. (a) Snapshot of phases of all junctions in a polar plot, and (b) their spatiotemporal dynamics confirming chimeralike states ($K = 0.49$). Red circles and the black line represent incoherent and coherent subpopulations, respectively, in (a).

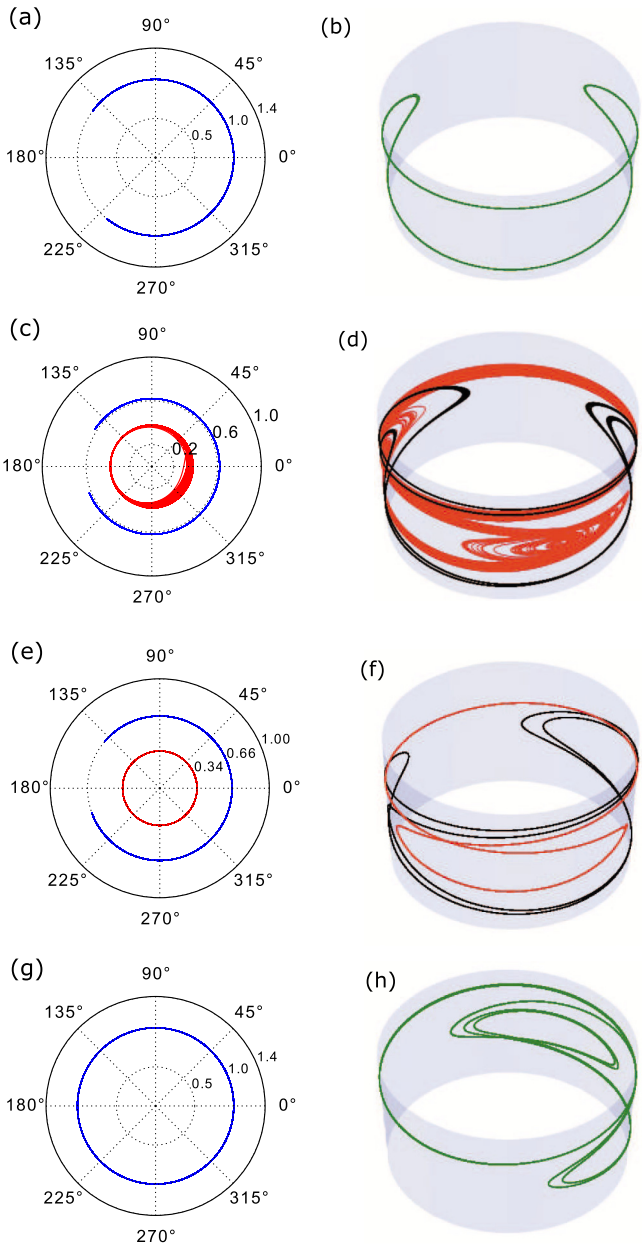

FIG. 4. r-Φ plot (left column) and phase portrait (y vs ϕ) in cylindrical space (right column). (a), (b) Coherent libration for $K = 0.305$, (c), (d) chimeralike states for $K = 0.49$, (e), (f) cluster states of coexisting libration and rotational motion for $K = 0.523$, and (g), (h) coherent rotational motion for $K = 0.56$.

For a demonstration of the chimeralike states, we present ($K = 0.49$) a snapshot of phases of all the junctions in a polar plane in Fig. 3(a). The incoherent subpopulation is clear from the distribution of phases of individual junctions (red circles) and the coherent junctions are aligned along the black line. The spatiotemporal dynamics of the voltage variable (y) of all the junctions is plotted in Fig. 3(b) for a long run that further confirms the existence of chimeralike states, the coexisting coherent and incoherent subpopulations.

Figure 4 describes the dynamical characters in different collective states (two coherent states, the clustered state and chimeralike states) of the junctions in r-Φ plots (left column) and their phase portraits in cylindrical space (right column). In the lower range of $K < 0.451$ (cf. Fig. 2), the coherent or single cluster dynamics of the junctions is librational ($l = 0$, $s = 0$) when the r-Φ plot in Fig. 4(a) shows an incomplete rotation (blue line, $r = 1$), and it is confirmed by its trajectory (green line) in a cylindrical space in Fig. 4(b). In contrast, the coherent or single cluster dynamics of the junctions at the other end (cf. Fig. 2) for larger $K > 0.532$ is complete rotational ($l = 1$, $s = 0$), as shown in the r-Φ plot (blue/light gray line, $r = 1$) and its trajectory (green line) in cylindrical space in Figs. 4(g) and 4(h), respectively. In the intermediate range, $0.451 < K < 0.512$, l fluctuates ($0 < l < 1$) and almost exactly follows the r fluctuation ($0 < r < 1$), where r shows a decreasing trend (Fig. 2) and we observe the chimeralike states. In the chimeralike states, the coherent subpopulation is in librational motion (blue/light gray line, $r \approx 0.6 < 1$) and the incoherent subpopulation (red lines) coexists in rotational motion (red line, $r < 1$; around 0.2), as shown in the r-Φ plot in Fig. 4(c). In cylindrical space in Fig. 4(d), the trajectories of the coherent subpopulation (black line) confirm their regular librational motion and the incoherent (red lines) counterpart in chaotic rotational motion. In the range of $K = 0.512$–0.532, as mentioned earlier, the clustered states (cf. $s = 0$ in Fig. 2) are seen where both the r-Φ plot and the trajectory in cylindrical space in Figs. 4(e) and 4(f), respectively, confirm the existence of coexisting subpopulations in regular rotational ($r = 0.34$) and regular librational motion ($r = 0.66$). Initial conditions are given in [40].

In summary, we revisited an earlier study [36] on the collective dynamics of a globally coupled Josephson junction array under a common rf forcing where order and turbulent states were reported to coexist, although no categorical statement about the existence of chimeralike states was made. Our present numerical study confirmed that chimeralike states indeed existed there. Furthermore, we explored two important classes of coherent states, a librational motion and a rotational motion, and an interesting process of transition from one to the other via the successive emergence of chimeralike states and cluster states when the coupling strength was increased. This phenomenon of nontrivial transition was not limited to a particular set of parameters used earlier, but existed in a broader parameter range (a second example is presented in the Supplemental Material [39]). A variety of dynamics, libration and rotational motion, in the junction array and their collective states, was identified, in parameter space, using the Kuramoto order parameter (r) and by introducing two measures, a librational index (l) and a clustering index (s), which were illustrated in a cylindrical space.

S.K.D. and P.K.R. acknowledge support by the CSIR (India) under the Emeritus Scientist Scheme. A.M. is supported by the UGC India. H.A.C. and S.K.D. thank ICTP-SAIFR and FAPESP Grant No. 2011/11973-4 for partial support. P.L. acknowledges support by the FAPESP Grant No. 2014/13272-1. S.S. acknowledges support by the DST (India) and C.H. is supported by the CHE/PBC, Israel.

[1] Y. Kuramoto and D. Battogtokh, Nonlinear Phenom. Complex Syst. **5**, 380 (2002).
[2] D. M. Abrams and S. H. Strogatz, Phys. Rev. Lett. **93**, 174102 (2004); D. M. Abrams, R. E. Mirollo, S. H. Strogatz, and D. A. Wiley, *ibid.* **101**, 084103 (2008).
[3] E. A. Martens, C. R. Laing, and S. H. Strogatz, Phys. Rev. Lett. **104**, 044101 (2010).
[4] G. C. Sethia, A. Sen, and F. M. Atay, Phys. Rev. Lett. **100**, 144102 (2008).
[5] I. Omelchenko, Y. L. Maistrenko, P. Hövel, and E. Schöll, Phys. Rev. Lett. **106**, 234102 (2011).
[6] I. Omelchenko, O. E. Omelchenko, P. Hövel, and E. Schöll, Phys. Rev. Lett. **110**, 224101 (2013).
[7] J. H. Sheeba, V. K. Chandrasekar, and M. Lakshmanan, Phys. Rev. E **79**, 055203 (2009); **81**, 046203 (2010).
[8] G. C. Sethia, A. Sen, and G. L. Johnston, Phys. Rev. E **88**, 042917 (2013).
[9] C. Gu, G. St-Yves, and J. Davidsen, Phys. Rev. Lett. **111**, 134101 (2013).
[10] A. Zakharova, M. Kapeller, and E. Schöll, Phys. Rev. Lett. **112**, 154101 (2014).
[11] L. Larger, B. Penkovsky, and Y. Maistrenko, Phys. Rev. Lett. **111**, 054103 (2013).
[12] D. Dudkowski, Y. Maistrenko, and T. Kapitaniak, Phys. Rev. E **90**, 032920 (2014).
[13] L. Schmidt and K. Krischer, Phys. Rev. Lett. **114**, 034101 (2015).
[14] N. Semenova, A. Zakharova, V. Anishchenko, and E. Schöll, Phys. Rev. Lett. **117**, 014102 (2016).
[15] S. L. Bressler and J. A. S. Kelso, Trends Cognit. Sci. **5**, 26 (2001); K. Friston, NeuroImage **5**, 164 (1997).
[16] M. R. Tinsley, S. Nkomo, and K. Showalter, Nat. Phys. **8**, 662 (2012).
[17] A. Hagerstrom, T. E. Murphy, R. Roy, P. Hövel, I. Omelchenko, and E. Schöll, Nat. Phys. **8**, 658 (2012).
[18] E. A. Martens, S. Thutupallic, A. Fourrierec, and O. Hallatscheka, Proc. Natl. Acad. Sci. U.S.A. **110**, 10563 (2013).
[19] K. Kaneko, Physica D **41**, 137 (1990); Chaos **25**, 097608 (2015).
[20] A. Yeldesbay, A. Pikovsky, and M. Rosenblum, Phys. Rev. Lett. **112**, 144103 (2014).
[21] G. C. Sethia and A. Sen, Phys. Rev. Lett. **112**, 144101 (2014).

[22] A. Mishra, C. Hens, M. Bose, P. K. Roy, and S. K. Dana, Phys. Rev. E **92**, 062920 (2015).
[23] C. R. Hens, A. Mishra, P. K. Roy, A. Sen, and S. K. Dana, Pramana **84**, 229 (2015).
[24] B. K. Bera, D. Ghosh, and M. Lakshmanan, Phys. Rev. E **93**, 012205 (2016).
[25] N. Lazarides, G. Neofotistos, and G. P. Tsironis, Phys. Rev. B **91**, 054303 (2015); J. Hizanidis, N. Lazarides, and G. P. Tsironis, Phys. Rev. E **94**, 032219 (2016).
[26] M. Wickramasinghe and I. Z. Kiss, PLoS One **8**, e80586 (2013).
[27] M. Levi, F. C. Hoppensteadt, and W. L. Miranker, Q. Appl. Math. **36**, 167 (1978).
[28] S. Strogatz, *Nonlinear Dynamics and Chaos* (Westview Press, Boulder, CO, 2015).
[29] C. Hens, P. Pal, and S. K. Dana, Phys. Rev. E **92**, 022915 (2015); T. Hongray, J. Balakrishnan, and S. K. Dana, Chaos **25**, 123104 (2015).
[30] S. K. Dana, D. C. Sengupta, and C.-K. Hu, IEEE Trans. Circuits Syst., II **53**, 1031 (2006); S. K. Dana, P. K. Roy, D. C. Sengupta, G. Sethia, and A. Sen, IEE Proc. Circuits Syst. Devices **153**, 453 (2006); S. K. Dana, D. C. Sengupta, and K. Edoh, IEEE Trans. Circuits Syst., I **48**, 990 (2001).
[31] J. Borresen and S. Lynch, PLoS One **7**, e48498 (2012).
[32] P. Crotty, D. Schult, and K. Segall, Phys. Rev. E **82**, 011914 (2010).
[33] V. Vlasov and A. Pikovsky, Phys. Rev. E **88**, 022908 (2013).
[34] K. Wiesenfeld, P. Colet, and S. H. Strogatz, Phys. Rev. Lett. **76**, 404 (1996).
[35] S. Watanabe and S. H. Strogatz, Physica D **74**, 197 (1994).
[36] D. Dominguez and H. A. Cerdeira, Phys. Rev. Lett. **71**, 3359 (1993); Phys. Rev. B **52**, 513 (1995); F. Xie and H. A. Cerdeira, Int. J. Bifurcation Chaos Appl. Sci. Eng. **8**, 1713 (1998).
[37] The natural phase space of the trajectory of a Josephson junction is cylindrical. We wrap up the phase space on a cylinder. In this phase space, the periodic behavior of the phase is more explicit. The radius of the cylinder (ρ) is taken as unity and its relation to the Cartesian coordinate is given by $x_1 = \rho\cos\phi$, $x_2 = \rho\sin\phi$, and $x_3 = y$.
[38] Y. Kuramoto, *Chemical Oscillations, Waves, and Turbulence* (Springer, New York, 1984).
[39] See Supplemental Material at http://link.aps.org/supplemental/10.1103/PhysRevE.95.010201 for a more detailed explanation of how the clustering index (s) and libration index (l) are defined.
[40] For the network of resistively and capacitively shunted junctions (RCSJs), we construct general V-shaped initial states for y_i between "range1" and "range2" as $y_{i0} = \text{range1} + (\text{range2} - \text{range1})(2\frac{i}{N})$ for $1 \leqslant i \leqslant \frac{N}{2}$ and $y_{i0} = \text{range1} - (\text{range2} - \text{range1})(2\frac{i}{N} - 2)$ for $\frac{N}{2} + 1 \leqslant i \leqslant N$ with added small random fluctuations. All initial states for ϕ variables are set at zero. For our simulation we chose range1 $= 2.0$ and range2 $= -2.0$.